LUND UNIVERSITY

The G protein-coupled oestrogen receptor 1 agonist G-1 disrupts endothelial cell microtubule structure in a receptor-independent manner.

Holm, Anders; Grände, Per-Olof; Ludueña, Richard F; Olde, Björn; Prasad, Veena; Leeb-Lundberg, Fredrik; Nilsson, Bengt-Olof

Published in:
Molecular and Cellular Biochemistry

DOI:
10.1007/s11010-012-1301-3

2012

Link to publication

Citation for published version (APA):
Holm, A., Grände, P.-O., Ludueña, R. F., Olde, B., Prasad, V., Leeb-Lundberg, F., & Nilsson, B.-O. (2012). The G protein-coupled oestrogen receptor 1 agonist G-1 disrupts endothelial cell microtubule structure in a receptor-independent manner. *Molecular and Cellular Biochemistry*, *366*(1-2), 239-249. https://doi.org/10.1007/s11010-012-1301-3

Total number of authors:
7

General rights
Unless other specific re-use rights are stated the following general rights apply:
Copyright and moral rights for the publications made accessible in the public portal are retained by the authors and/or other copyright owners and it is a condition of accessing publications that users recognise and abide by the legal requirements associated with these rights.
• Users may download and print one copy of any publication from the public portal for the purpose of private study or research.
• You may not further distribute the material or use it for any profit-making activity or commercial gain
• You may freely distribute the URL identifying the publication in the public portal

Read more about Creative commons licenses: https://creativecommons.org/licenses/

Take down policy
If you believe that this document breaches copyright please contact us providing details, and we will remove access to the work immediately and investigate your claim.

LUND UNIVERSITY

PO Box 117
221 00 Lund
+46 46-222 00 00

The G protein-coupled estrogen receptor 1 agonist G-1 disrupts endothelial cell microtubule structure in a receptor-independent manner

Anders Holm[a], Per-Olof Grände[b], Richard F. Ludueña[c], Björn Olde[a], Veena Prasad[c], L. M. Fredrik Leeb-Lundberg[a], Bengt-Olof Nilsson[a]*

[a]Department of Experimental Medical Science, Lund University, BMC D12, SE-221 84 Lund, Sweden
[b]Department of Clinical Science, Lund University and Lund University Hospital, BMC F11, SE-221 84 Lund, Sweden
[c]Department of Biochemistry, University of Texas Health Science Center at San Antonio 7703 Floyd Curl Drive, San Antonio, Texas 78229-3900, USA

***Corresponding author:**

Dr. Bengt-Olof Nilsson
Department of Experimental Medical Science
Lund University
BMC D12
SE-221 84 Lund
Sweden
Phone:+46-46-2227767
Fax: +46-46-2224546
E-mail: bengt-olof.nilsson@med.lu.se

Abstract

The G protein-coupled estrogen receptor GPER1, also known as GPR30, has been implicated in estrogen signalling, but the physiological importance of GPER1 is not fully understood. The GPER1 agonist G-1 has become an important tool to assess GPER1-mediated cellular effects. Here, we report that this substance, besides acting via GPER1, affects the microtubule network in endothelial cells. Treatment with G-1 (3 µM) for 24 h reduced DNA synthesis by about 60% in mouse microvascular endothelial bEnd.3 cells. Treatment with 3 µM G-1 prevented outgrowth of primary endothelial cells from mouse aortic explants embedded in Matrigel. Treatment with G-1 (0.3-3 µM) for 24 h disrupted bEnd.3 cell and HUVEC microtubule structure in a concentration-dependent manner as assessed by laser-scanning confocal immunofluorescence microscopy. G-1-induced (3 µM) disruption of microtubule was observed also after acute (3 and 6 h) treatment and in the presence of the protein synthesis inhibitor cycloheximide. Disruption of microtubules by 3 µM G-1 was observed in aortic smooth muscle cells obtained from both GPER1 knockout and wild-type mice, suggesting that G-1 influences microtubules through a mechanism independent of GPER1. G-1 dose-dependently (10-50 µM) stimulated microtubule assembly in-vitro. On the other hand, microtubules appeared normal in the presence of 10-50 µM G-1 as determined by electron microscopy. We suggest that G-1-promoted endothelial cell anti-proliferation is due in part to alteration of microtubule organization through a mechanism independent of GPER1. This G-1-promoted mechanism may be used to block unwanted endothelial cell proliferation and angiogenesis such as that observed in e.g. cancer.

Keywords: endothelial cells; G-1; GPR30; microtubule; proliferation; tubulin

Introduction

Two estrogen receptors, ERα and ERβ, have been identified [1-3]. The G protein-coupled estrogen receptor 1 (GPER1), previously known as G protein-coupled receptor 30 (GPR30), was recently suggested to represent a new estrogen receptor [4, 5]. ERα, ERβ and GPER1 show tissue-specific expression patterns [6-11]. Estrogen exerts atheroprotective effects via different mechanisms including attenuation of vascular smooth muscle cell proliferation in response to vascular injury and stimulation of endothelial NO formation, mechanisms which have been reported to be mediated through ERα activation [12-16]. Estrogen also reduces vascular inflammation and promotes vascular re-endothelialisation; the latter effect has been attributed to ERα, offering additional possible estrogen-promoted atheroprotective mechanisms [17, 18]. Thus, several studies suggest an important role for vascular ERα, whereas much less information is available regarding the role of vascular ERβ and GPER1.

Mouse carotid and mesenteric arteries express GPER1 mRNA [9, 19], and GPER1 immunoreactivity has been demonstrated in both intima and media of rat aorta, which suggest that both endothelial and vascular smooth muscle cells express GPER1 [20]. Furthermore, Isensee *et al.* [8] used LacZ reporter mice to show different degrees of GPER1 expression in different vessels ranging from no expression in large vessels to high GPER1 expression in the endothelium of small arteries and in the Vasa vasorum of the outer layers of the aorta.

A GPER1 agonist, named G-1 (formal name: rel-1-[4-(6-bromo-1,3-benzodioxol-5-yl)-3aR,4S,5,9bS-tetrahydro-3H-cyclopenta[c]quinolin-8-yl]-ethanone; molecular formula: $C_{21}H_{18}BrNO_3$), was recently developed [21]. Treatment with G-1 has been reported to attenuate blood pressure in both normotensive rats and in ovariectomized MREN2.LEWIS

rats [19, 20]. Besides reducing blood pressure, G-1 has been demonstrated to reduce both vascular smooth muscle cell and endothelial cell proliferation [19, 22]. The G-1-induced endothelial cell anti-proliferative effect involves attenuation of DNA synthesis through a GPER1-dependent mechanism as well as arrest in S and G2 phases of the cell cycle [22]. Treatment with μM concentrations of G-1 has a dramatic anti-proliferative effect reducing endothelial cell DNA synthesis by 60-90% with an IC_{50} value of 1.9 μM for G-1-induced inhibition of DNA synthesis, suggesting that this agent may be used to inhibit angiogenesis [22]. However, besides reducing endothelial cell proliferation by inhibition of DNA synthesis via a GPER1-dependent mechanism, G-1 may also cause endothelial cell anti-proliferation via other mechanisms, e.g. by disruption of tubulin polymerisation/depolymerisation in a similar way to that of the well-known anti-cancer drugs paclitaxel (taxol), vincristine, and vinblastine [23].

The objective of the present study was to investigate the effects of the GPER1 agonist G-1 on microtubule structure in endothelial cells and its mechanisms of action. We disclose here that μM concentrations of G-1 reduce endothelial cell proliferation and disrupt microtubule network structure through a GPER1-independent mechanism, suggesting that G-1 may be used to reduce and/or prevent unwanted formation of new blood vessels as observed in e.g. cancer through this mechanism.

Materials and methods

Cell culture

The mouse brain microvascular endothelial cell line (bEnd.3) was purchased from American Type Tissue Culture Collection (ATCC, Manassas, VA, USA) and cultured in Dulbecco's modified Eagle's medium supplemented with 10% foetal calf serum (FCS) and antibiotics (penicillin 100 U/ml, streptomycin 100 μg/ml). Human umbilical vein endothelial cells (HUVEC) were purchased from Lonza (Lonza, Walkersville, MD, USA) and cultured in endothelial cell culture medium as recommended by Lonza. The cells were used in passages 2-5. The bEnd.3 cells express the endothelial cell marker protein eNOS in passages 2-5 [24, 25]. Furthermore, they express ERα, ERβ and GPER1 [22] confirming the estrogen receptor expression pattern observed in endothelial cells in-vivo [8, 26]. The HUVECs are primary endothelial cells validated by expression of the endothelial cell markers von Willebrand Factor, CD31 and CD105. Cell culture dishes were placed in a water-jacketed cell incubator at 37°C in 5% CO_2 in air. Before experiments normal culture medium was replaced with phenol red-free and FCS-free culture medium for 24 h to make cells quiescent and to remove the estrogen-like activity of phenol red. The phenol red-free culture medium was used throughout the experiment. Experiments were performed using dextran-coated charcoal stripped FCS. Dextran-coated charcoal was used to remove steroids from normal FCS. Cell viability was assessed by trypan-blue exclusion test. After removing cell culture medium cells were washed with NaCl (0.9%) and then incubated for 2 min with 0.4% trypan-blue (Sigma Chemicals, St Louis, MO, USA). The cells were washed three times and then the number of cells containing trypan-blue was counted as a measure of dead/dying cells.

Culture of primary vascular smooth muscle cells from GPER1 knockout and wild-type mice

GPER1/GPR30 (-/-) mice were generated as described previously by Mårtensson *et al*. [9]. For these experiments female mice were used and age-matched wild-type C57BL/6 female mice served as controls. Knockout of the GPER1 gene was confirmed by PCR (Fig. 1). For genotyping of the mice the following GPER1 primer pair was employed: forward, GATCGTTAGATTAACAGAGCAG; reverse, CCTGGGAGCCTGTTAGTCTCAG. This primer pair produces a GPER1 specific product [9]. The animals were kept under standardized conditions with food and water ad libitum and a 12 h light/dark cycle. The animal experiments were approved by the Animal Ethics Committee at Lund University. The GPER1 knockout and wild-type animals were killed by cervical dislocation and then the aorta was dissected free from blood, fat and connective tissue. The aorta was cut into rings of identical width (0.5 mm) under a dissecting microscope and 5 aortic rings were placed in each cell culture dish containing Dulbecco's modified Eagle's medium, supplemented with 10% FCS and antibiotics (penicillin100 U/ml, streptomycin 100 µg/ml). The dishes were placed in a cell incubator at 37 °C under 5% CO_2 in air. Vascular smooth muscle cells were allowed to grow out from the tissue explants and at day 10 the aortic rings were removed. The cells were trypsinized upon reaching confluence and seeded on glass cover slips for assessment of microtubule and smooth muscle α actin. The cells expressed the smooth muscle cell marker smooth muscle α actin showing that they represent vascular smooth muscle cells.

Outgrowth of endothelial cells from aortic rings embedded in Matrigel

In order to study effects of G-1 on outgrowth of endothelial cells from arterial rings we incubated aortic rings from female wild-type and GPER1 knockout mice for 8 days with or

without G-1 in Matrigel (Matrigel™ Phenol red-free, BD, Franklin Lakes, NJ, USA). The aorta was dissected free from blood, fat and connective tissue. The vessel was then cut into rings of identical width (0.5 mm) under a dissecting microscope. The aortic rings were mounted in cell culture dishes with Matrigel with phenol red-free DMEM cell culture medium supplemented with 10% dextran-coated charcoal stripped FCS and antibiotics and treated with or without G-1 for 8 days. The dishes were placed in a cell incubator at 37 °C under 5% CO_2 in air. The cells growing out from explants embedded in Matrigel were elongated and arranged in long rows resembling tubes. Cell proliferation in Matrigel was evaluated by counting the number of cells migrating out of the aortic explants between 4 and 8 days after embedding. Cell counting was performed by phase contrast microscopy using an Olympus CK40 microscope (Olympus Europa GmbH, Hamburg, Germany).

DNA synthesis measurement

DNA synthesis was determined by measuring incorporation of [^{3}H] thymidine. The isotope was included for the last hour of the 24 h incubation. The cells were washed in PBS and then harvested using a rubber policeman. Cells were sonicated in 5 mM NaOH twice for 10 s. Aliquots of the sonicate was precipitated with 5% trichloroacetic acid and centrifuged (10621 g for 2 min at 4 ˚C). After washing with trichloroacetic acid (5%) the pellet was dissolved in soluene. Liquid scintilliation cocktail was added and radioactivity measured in a liquid scintilliation counter (Beckman, Fullerton, CA, USA). Radioactivity was expressed as disintegrations per minute (D.P.M.) and normalised to the concentration of total protein in each sample. Protein concentration was determined by using a Bio-Rad protein assay kit (Bio-Rad, Hercules, CA, USA) based on the Lowry method [27].

Quantitative real-time PCR

Total RNA was extracted and purified using RNeasy Mini Kit (Qiagen, Valencia, CA, USA). Concentration and purity of RNA was measured at 260/280 nm in a NanoDrop ND-100 spectrophotometer (NanoDrop Technologies Inc., Wilmington, DE, USA). The RNA samples were then subjected to one-step quantitative real-time PCR measurements using QuantiFast SYBR Green RT-PCR kit (Qiagen) and QuantiTect primer assays (Qiagen) on a Step One Plus real-time thermal cycler from Applied Biosystems (Applied Biosystems, Foster City, CA, USA). Each sample was analyzed in duplicate. Gene expression was calculated using the delta CT method as described by Pfaffl [28]. The RNA samples were used for quantitative RT-PCR measurements applying glyceraldehyde-3-phosphate dehydrogenase (GAPDH), 18S ribosomal RNA (18S) and peptidylprolyl isomerase A (Ppia) as house-keeping reference genes. Identical results were obtained when target gene expression was normalized to GAPDH, 18S and Ppia. All three house-keeping genes were unaffected by G-1 treatment. Data presented in results section are normalized to GAPDH. The PCR primers (QuantiTect Primer Assays) for VEGF-A (Mm_Vegfa_1_SG), VEGFR1 (Mm_Flt1_1_SG), VEGFR2 (Mm_Kdr_1_SG), GAPDH (Mm_Gapdh_3_SG), 18S (Mm_Rn18s_2_SG) and Ppia (Mm_Ppia_1_SG) were purchased from Qiagen.

Microtubule staining

Cells were cultured on glass cover slips and fixed in 4% paraformaldehyde for 10 min at room temperature. The cells were then washed carefully in PBS and microtubule was assessed by immunocytochemistry using a mouse monoclonal α-tubulin antibody (Sigma) at 1:4000 dilution. Immunofluorescence was visualized using a Cy3-conjugated secondary anti-mouse

antibody at 1:500 dilution (Invitrogen, Carlsbad, CA, USA). The glass cover slips with cells stained for α-tubulin were carefully washed and mounted on microscope slides. Fluorescence was analyzed using a laser-scanning confocal microscope (LSM 510 PASCAL, Carl Zeiss AG, Göttingen, Germany). Digital photos were analyzed in a blinded fashion.

Microtubule assembly assay and microtubule electron microscopy

Microtubule protein was prepared from bovine cerebra by the cycling method of Fellous *et al*. [29]. Microtubule protein consists of tubulin and various microtubule associated proteins (MAPs), specifically MAP1A, MAP1B, MAP2 and tau. Microtubule assembly was monitored at 37 ºC in a Beckman DU 7400 model spectrophotometer equipped with an automatic cuvette programmer (Beckman, Fullerton, CA, USA). Microtubules (2 mg/ml) were assembled in the presence and absence of G-1. G-1 was dissolved in dimethylsulfoxide (DMSO) and an equivalent amount of DMSO was added to the control. Cuvette temperature was controlled using a Beckman Thermoset. Assembly experiments were done in the following buffer: 0.1 M MES, pH 6.4, 1 mM EGTA, 0.1 mM EDTA, 1 mM GTP, and 0.5 mM $MgCl_2$.

Electron microscopy was done according to Olmsted and Borisy [30] with little modification. After microtubule assembly, the assembled mixture was diluted with an equal volume of 50% (w/v) sucrose in assembly buffer. Twenty µl of this mixture was placed on a 200-mesh copper grid coated with formvar and carbon and was allowed to adsorb for 1 min. The grid was successively washed with three drops of each of the following: (a) 1 mg/ml cytochrome c in water, (b) water, and (c) 1% uranyl acetate in water. Excess solutions were soaked off with a blotting paper. The grids were air-dried and examined under a Jeol 100CX electron microscope (Jeol Ltd., Tokyo, Japan) at an accelerating voltage of 60 kv. Protein

determination was done according to the method of Lowry *et al*. [27] as modified by Schachterle and Pollack [31].

Drugs

G-1 was purchased from Cayman Chemical, Ann Arbor, MI, USA and dissolved in dimethylsulfoxide (DMSO, Sigma). Cycloheximide was from Sigma and dissolved in PBS. Controls received DMSO as vehicle. The final concentration of DMSO was 0.1-0.3 %.

Statistics

Summarized data are presented as means ±S.E.M. Statistical significance was calculated using ANOVA and Mann-Whitney U test for unpaired comparison with Bonferroni correction for post-hoc analysis as appropriate. P-values less than 0.05 were regarded as denoting statistical significance.

Results

Effects of G-1 on bEnd.3 cell DNA synthesis and VEGF-A, VEGFR1 and VEGFR2 expression

Treatment of bEnd.3 cells with 3 μM G-1 reduced basal (0% FCS) DNA synthesis by about 60% (Fig. 2), whereas lower concentrations of G-1 (0.3 and 1 μM) had no significant effect (Fig. 2). We previously reported that G-1 (3 μM) attenuates endothelial cell DNA synthesis also under growth-stimulated conditions (5% FCS) [22]. Thus, G-1 seems to reduce DNA synthesis under growth-arrested as well as growth-stimulated conditions. Next, we investigated the effects of G-1 on pro-angiogenic VEGF-A expression and the expression of its receptors VEGFR1 and VEGFR2 [32] in bEnd.3 cells under growth-stimulated conditions (10% stripped FCS). Treatment with G-1 (3 μM) for 48 h had no effect on VEGF-A mRNA expression (0.96 ± 0.18 in G-1-treated cells vs. 1.04 ± 0.16 in control cells, n=5 and 6). Also, treatment with G-1 for a shorter time (16 h) had no effect on VEGF-A transcript expression (1.09 ± 0.10 in G-1-treated cells vs. 1.00 ± 0.03 in control cells, n=12 in each group). Furthermore, treatment with G-1 (3 μM) for 16 h had no effect on the mRNA levels of either VEGFR1 (0.80 ± 0.10 in G-1-treated cells vs. 1.00 ± 0.04 in control cells, n=6 in each group) or VEGFR2 (1.06 ± 0.27 in G-1-treated cells vs. 1.15 ± 0.31 in control cells, n=6 in each group). Thus, the G-1-induced inhibition of endothelial cell proliferation was not associated with decreased expression of mRNA for either VEGF-A, VEGFR1, or VEGFR2, suggesting that G-1-promoted anti-proliferation is not mediated via the VEGF pathway, although we cannot rule out the possibility that G-1 acts down-stream of the VEGFR.

Effects of G-1 on outgrowth of endothelial cells from aortic explants in Matrigel

Aortic rings from female mice were embedded in Matrigel in order to study the effect of G-1 on primary endothelial cell sprouting. Cells growing out from the aortic explants embedded in Matrigel were elongated and formed contact with each other establishing tube-like structures. Cells were observed around the aortic explants embedded in Matrigel within 4 days. Treatment of the rings in Matrigel with 3 μM G-1, under growth-stimulated conditions (10 % stripped FCS), prevented cellular-outgrowth recorded 4-8 days after embedding (Fig. 3A). A lower G-1 concentration (1 μM) had no effect (Fig. 3A). Treatment with 3 μM G-1 prevented outgrowth of endothelial cells from aortic rings derived from both wild-type and GPER1-deficient mice (Fig. 3B). The anti-angiogenic effect of G-1 was reversed, i.e. new cells were observed around the embedded explants, within 4 days after replacement of the G-1-containing medium with fresh medium without G-1. No or very few trypan-blue containing cells were observed after trypan-blue staining of aortic endothelial cells treated either with or without 3 μM G-1 indicating high cell viability.

Effects of G-1 on endothelial cell microtubule structure

Treatment with G-1 (3 μM) for 24 h under growth-stimulated culture conditions (10% stripped FCS) drastically altered the bEnd.3 cell microtubule network structure as assessed by α-tubulin immunocytochemistry and laser-scanning confocal fluorescence microscopy (Fig. 4). G-1 altered the structure of the microtubule filaments from long and continuous threads in control cells to short and disrupted ones in G-1 treated cells (Fig. 4). Besides causing disruption of microtubule filaments, G-1 also caused sharp bends and hooks of the filaments (Figs. 4-6). The number of alterations assessed by counting sharp bends and hooks in the G-1 treated cells were compared to those in untreated cells (Figs. 5A and B). The G-1-promoted

effect was also observed at lower (0.3 and 1 μM) concentrations (Fig. 5A). In addition, alteration of microtubule filaments similar to that observed in bEnd.3 cells was observed in response to 0.3-3 μM G-1 in HUVECs as well (Fig. 5B). As demonstrated in figures 5A and 5B, the G-1-promoted alteration of endothelial cell microtubules was concentration-dependent. Not only 24 h treatment but also treatment with 3μM G-1 for shorter time points, i.e. 3 and 6 h, altered the microtubule structure causing sharp bends and hooks of the filaments (Fig. 6). Treatment with 3 μM G-1 for 15 and 30 min had no effects on microtubule structure (data not shown). As demonstrated in figure 7, treatment with G-1 (3 μM) for 24 h altered microtubule structure also in the presence of the protein synthesis inhibitor cycloheximide (50 μg/ml). The concentration of cycloheximide used here is the same one as previously used to inhibit protein synthesis studying protein turnover [33].

Effects of G-1 on microtubule structure in aortic smooth muscle cells from wild-type and GPER1 knockout mice

In order to investigate the involvement of GPER1 in mediating the G-1-induced disruption of microtubule, aortic smooth muscle cells were obtained from GPER1 knockout female mice and age-matched wild-type female mice. Treatment with 3 μM G-1 for 24 h under growth-stimulated culture conditions (10% stripped FCS) disrupted microtubule in aortic smooth muscle cells derived from both wild-type and GPER1-deficient mice, suggesting that G-1-induced perturbation of the microtubule network is mediated via a mechanism independent of GPER1 (Fig. 8). On the other hand, the microtubule network structure was similar in control aortic smooth muscle cells not treated with G-1 obtained from GPER1-deficient and wild-type mice (Fig. 8).

Effects of G-1 on microtubule assembly and microtubule structure in-vitro

Microtubules were allowed to polymerize in the presence of a series of concentrations of G-1. The drug enhanced the rate and extent of microtubule assembly in a concentration-dependent fashion at 10 to 50 μM (Fig. 9). A lower concentration of G-1 (1 μM) had no effect on microtubule assembly (data not shown). Examination of the polymerized microtubule by electron microscopy showed normal fairly straight microtubules in the absence as well as in the presence of 10-50 μM G-1 (data not shown). No wavy microtubules were seen by this analysis.

Discussion

Here, we show that the GPER1 agonist G-1 has a pronounced inhibitory effect on endothelial cell proliferation and disrupts microtubules in endothelial cells. G-1 alters endothelial cell microtubule network structure causing disruption and sharp bends of the microtubule filaments in a concentration-dependent manner between 0.3 and 3 µM showing dramatic derangement of the microtubule network at 3 µM, whereas inhibition of DNA synthesis by G-1 is observed at 3 µM but not at lower concentrations. Assuming that microtubule disruption and anti-proliferation are related, these results suggest that disruption of microtubules by G-1 needs to reach a threshold before proliferation is retarded. G-1-induced disruption of microtubule is observed in cells derived from both GPER1 knockout and wild-type mice suggesting that G-1 disrupts microtubules through a mechanism independent of GPER1. This mechanism may involve a different cellular signalling pathway besides GPER1, or a direct molecular interaction with tubulin or microtubule-associated proteins (MAPs). Not only 24 h incubation with G-1 but also treatment for shorter time-points, i.e. 3 and 6 h, alters endothelial cell microtubule structure, suggesting that G-1 acts independent of transcriptional and translational mechanisms. More acute incubation with G-1 (i.e. 15 and 30 min) had no effect on microtubule structure, suggesting that G-1 needs at least this time to interact with its molecular targets. G-1-induced alteration of microtubule structure is observed also in the presence of the protein synthesis inhibitor cycloheximide, providing further evidence for a mechanism independent of transcription and translation.

Our data show that G-1 affects microtubule assembly in-vitro. The effect is to enhance microtubule assembly although the concentrations required for the effect in-vitro are significantly higher than those that cause formation of wavy or hook-shaped microtubules in-

vivo. It is not clear how enhancement of microtubule assembly in-vitro translates into the highly curved microtubules in-vivo. The most likely explanation is that the two effects are unrelated. It is possible that in-vitro G-1 interacts directly with tubulin, although with low affinity. It is also possible that G-1 interacts with MAPs in some fashion so as to enhance microtubule assembly indirectly. Structurally, G-1 has a slight resemblance to estramustine phosphate, which has been reported to inhibit microtubule assembly in-vitro by binding to MAPs [34]. Therefore, it is possible that G-1 enhances microtubule assembly in-vitro by binding to one or more of the MAPs present in the microtubule protein. One could hypothesize that one drug binds to a MAP and affects its conformation in a certain way so as to enhance its interaction with tubulin, while the other drug binds to a MAP and affects its conformation so as to inhibit its interaction with tubulin. How G-1 causes formation of curved microtubules in-vivo is still not clear. Such extreme curvature of microtubules appears to be relatively novel. An interesting observation by Dhamodaran *et al*. [35] is that at very low concentrations, vinblastine can cause formation of wavy microtubules in-vivo, although not as curved as the ones reported here, but that at higher concentrations of vinblastine, microtubules actually appear morphologically fairly normal, although somewhat shorter. In view of the results obtained in-vitro, it is very unlikely that G-1 exerts its effects in-vivo by binding directly to tubulin. But, the results presented here raise the possibility that it may bind to some type of microtubule-associated protein, perhaps similar but not identical to the MAPs that are found largely in the nervous system [36] and that the effect of G-1 binding to this putative MAP is that the latter now binds differently to microtubules and allows or causes them to assume a more wavy configuration.

Drugs binding to tubulin such as paclitaxel (taxol), vincristine, and vinblastine are important anti-cancer drugs acting by disruption of either polymerisation or depolymerisation of

microtubules thereby interfering with the formation of the mitotic spindle and blocking cancer cell proliferation through cell cycle arrest [23]. Here we present G-1 as a new microtubule-interfering drug showing powerful disruption of the microtubule structure in endothelial cells. Future studies investigating the anti-proliferative effects of G-1 in cancer cells and tumour models in-vivo are urgently needed. For inhibition of endothelial cell proliferation in whole animal experiments local concentrations of G-1 in the µM range are probably needed based on our findings in cultured cells. It might represent a major problem to achieve µM concentrations in experiments in whole animals, especially since G-1 is lipophilic and thus readily diffuses over the cell-membrane and accumulates intracellularly e.g. in adipocytes.

Proliferation of urinary bladder epithelial cells is also reduced by G-1 [37], but in this tissue G-1 seems to induce anti-proliferation at lower concentrations than those needed to achieve anti-proliferation in endothelial cells, which suggests that the anti-proliferative mechanism of G-1 depends on cell origin. Previous studies in urinary bladder epithelial cells and endothelial cells show that G-1 reduces DNA synthesis through a GPER1-dependent mechanism [22, 37]. Here, we show that G-1 acts anti-proliferative and disrupts microtubule independent of GPER1. Thus, G-1 seems to act anti-proliferative via both GPER1-dependent and GPER1-independent mechanisms. We show in the present study that G-1 disrupts the microtubule network in both mouse brain microvascular bEnd.3 endothelial cells and human umbilical vein HUVEC endothelial cells, showing that G-1 disrupts microtubule structure in endothelial cell lines of different origin.

In summary, we propose that µM concentrations of the GPER1 agonist G-1 cause endothelial cell anti-proliferation by disrupting the microtubule network structure through a GPER1-

independent mechanism, suggesting that G-1 may be used to block unwanted endothelial cell proliferation via this mechanism in angiogenesis such as that observed in e.g. cancer.

Acknowledgements

This study was supported by grants from the Swedish Research Council, the Swedish Dental Society, the Greta and Johan Kocks Foundation, the Sven and Lilly Thuréus Foundation, and the Vascular Wall Programme at Lund University. We thank Dr. Mary Ann Jordan of the University of California at Santa Barbara for her thoughtful advice. Supported in part by a grant to RFL from the United States Department of Defence Breast Cancer Research Program W81XWH-10-1-0903. RFL and VP gratefully acknowledge the support of the Cancer Therapy and Research Center at the University of Texas Health Science Center San Antonio, an NCI-designated Cancer Center.

References

1. Green S, Walter P, Kumar V, Krust A, Bornert JM, Argos P, Chambon P (1986) Human oestrogen receptor cDNA: sequence, expression and homology to v-erb-A. Nature 320:134-139

2. Greene GL, Gilna P, Waterfield M, Baker A, Hort Y, Shine J (1986) Sequence and expression of human estrogen receptor complementary DNA. Science 231:1150-1154

3. Kuiper GG, Enmark E, Pelto-Huikko M, Nilsson S, Gustafsson JA (1996) Cloning of a novel receptor expressed in rat prostate and ovary. Proc Natl Acad Sci USA 93:5925-5930

4. Revankar CM, Cimino DF, Sklar LA, Arterburn JB, Prossnitz ER (2005) A transmembrane intracellular estrogen receptor mediates rapid cell signaling. Science 307:1625-1630

5. Thomas P, Pang Y, Filardo EJ, Dong J (2005) Identity of an estrogen membrane receptor coupled to a G protein in human breast cancer cells. Endocrinology 146:624-632

6. Owman C, Blay P, Nilsson C, Lolait SJ (1996) Cloning of human cDNA encoding a novel heptahelix receptor expressed in Burkitt's lymphoma and widely distributed in brain and peripheral tissues. Biochem Biophys Res Commun 228:285-292

7. Nilsson S, Makela S, Treuter E, Tujague M, Thomsen J, Andersson G, Enmark E, Pettersson K, Warner M, Gustafsson JA (2001) Mechanisms of estrogen action. Physiol Rev 81:1535-1565

8. Isensee J, Meoli L, Zazzu V, Nabzdyk C, Witt H, Soewarto D, Effertz K, Fuchs H, Gailus-Durner V, Busch D, Adler T, de Angelis MH, Irgang M, Otto C, Noppinger PR (2009) Expression pattern of Gpr30 in LacZ reporter mice. Endocrinology 150:1722-1730

9. Martensson UE, Salehi SA, Windahl S, Gomez MF, Sward K, Daszkiewicz-Nilsson J, Wendt A, Andersson N, Hellstrand P, Grande PO, Owman C, Rosen CJ, Adamo ML, Lundquist I, Rorsman P, Nilsson BO, Ohlsson C, Olde B, Leeb-Lundberg LM (2009) Deletion of the G protein-coupled receptor 30 impairs glucose tolerance, reduces bone growth, increases blood pressure, and eliminates estradiol-stimulated insulin release in female mice. Endocrinology 150:687-698

10. Otto C, Fuchs I, Kauselmann G, Kern H, Zevnik B, Andreasen P, Schwarz G, Altmann H, Klewer M, Schoor M, Vonk R, Fritzemeier KH (2009) GPR30 does not mediate estrogenic responses in reproductive organs in mice. Biol Reprod 80:34-41

11. Olde B, Leeb-Lundberg LM (2009) GPR30/GPER1: searching for a role in estrogen physiology. Trends Endocrinol Metab 20:409-416

12. Chen Z, Yuhanna IS, Galcheva-Gargova Z, Karas RH, Mendelsohn ME, Shaul PW (1999) Estrogen receptor alpha mediates the nongenomic activation of endothelial nitric oxide synthase by estrogen. J Clin Invest 103:401-406

13. Darblade B, Pendaries C, Krust A, Dupont S, Fouque MJ, Rami J, Chambon P, Bayard F, Arnal JF (2002) Estradiol alters nitric oxide production in the mouse aorta through the alpha-, but not beta-, estrogen receptor. Circ Res 90:413-419

14. Pare G, Krust A, Karas RH, Dupont S, Aronovitz M, Chambon P, Mendelsohn ME (2002) Estrogen receptor-alpha mediates the protective effects of estrogen against vascular injury. Circ Res 90:1087-1092

15. Pendaries C, Darblade B, Rochaix P, Krust A, Chambon P, Korach KS, Bayard F, Arnal JF (2002) The AF-1 activation-function of ERalpha may be dispensable to mediate the effect of estradiol on endothelial NO production in mice. Proc Natl Acad Sci USA 99:2205-2210

16. Simoncini T, Hafezi-Moghadam A, Brazil DP, Ley K, Chin WW, Liao JK (2000) Interaction of oestrogen receptor with the regulatory subunit of phosphatidylinositol-3-OH kinase. Nature 407:538-541

17. Nilsson BO (2007) Modulation of the inflammatory response by estrogens with focus on the endothelium and its interactions with leukocytes. Inflamm Res 56:269-273

18. Toutain CE, Filipe C, Billon A, Fontaine C, Brouchet L, Guery JC, Gourdy P, Arnal JF, Lenfant F, 2009. Estrogen receptor alpha expression in both endothelium and hematopoietic cells is required for the accelerative effect of estradiol on reendothelialization. Arterioscler Thromb Vasc Biol 29:1543-1550

19. Haas E, Bhattacharya I, Brailoiu E, Damjanovic M, Brailoiu GC, Gao X, Mueller-Guerre L, Marjon NA, Gut A, Minotti R, Meyer MR, Amann K, Ammann E, Perez-Dominguez A, Genoni M, Clegg DJ, Dun NJ, Resta TC, Prossnitz ER, Barton M (2009) Regulatory role of G protein-coupled estrogen receptor for vascular function and obesity. Circ Res 104: 288-291

20. Lindsey SH, Cohen JA, Brosnihan KB, Gallagher PE, Chappell MC (2009) Chronic treatment with the Gpr30 agonist G-1 decreases blood pressure in ovariectomized Mren2.Lewis rats. Endocrinology 150:3753-3758

21. Bologa CG, Revankar CM, Young SM, Edwards BS, Arterburn JB, Kiselyov AS, Parker MA, Tkachenko SE, Savchuck NP, Sklar LA, Oprea TI, Prossnitz ER (2006) Virtual and biomolecular screening converge on a selective agonist for GPR30. Nat Chem Biol 2:207-212

22. Holm A, Baldetorp B, Olde B, Leeb-Lundberg LM, Nilsson BO (2011) The GPER1 agonist G-1 attenuates endothelial cell proliferation by inhibiting DNA synthesis and accumulating cells in the S and G2 phases of the cell cycle. J Vasc Res 48:327-335

23. Schwartz EL (2009) Antivascular actions of microtubule-binding drugs. Clin Cancer Res 15:2594-2601

24. Bevers LM, Braam B, Post JA, van Zonneveld, AJ, Rabelink TJ, Koomans HS, Verhaar MC, Joles JA (2006) Tetrahydrobiopterin, but not L-arginine, decreases NO synthase uncoupling in cells expressing high levels of endothelial NO synthase. Hypertension 47:87-94

25. Odenlund M, Ekblad E, Nilsson BO (2008) Stimulation of oestrogen receptor-expressing endothelial cells with oestrogen reduces proliferation of cocultured vascular smooth muscle cells. Clin Exp Pharmacol Physiol 35:245-248

26. Andersson C, Lydrup ML, Ferno M, Idvall I, Gustafsson JA, Nilsson BO (2001) Immunocytochemical demonstration of oestrogen receptor β in blood vessels of the female rat. J Endocrinol 169:241-247

27. Lowry OH, Rosebrough NJ, Farr AL, Randall RJ (1951) Protein measurement with the Folin phenol reagent. J Biol Chem 193:265-275

28. Pfaffl MW (2001) A new mathematical model for relative quantification in real-time RT-PCR. Nucleic Acids Res 29:e45

29. Fellous A, Francon J, Lennon AM, Nunez J (1977) Microtubule assembly in vitro: purification of assembly-promoting factors. Eur J Biochem 78:167-174

30. Olmsted JB, Borisy GG (1973) Characterization of microtubule assembly in porcine brain extracts by viscometry. Biochemistry 12:4282-4289

31. Schacterle GR, Pollack RL (1973) A simplified method for the quantitative assay of small amounts of protein in biologic material. Anal Biochem 51:654-655

32. Eilken HM, Adams RH (2010) Dynamics of endothelial cell behavior in sprouting angiogenesis. Curr Opin Cell Biol 22:617-625

33. Batonnet S, Leibovitch MP, Tintignac L, Leibovitch SA (2004) Critical role for lysine 133 in the nuclear ubiquitin-mediated degradation of MyoD. J Biol Chem 279:5413-5420

34. Wallin M, Deinum J, Fridén B (1985) Interaction of estramustine phosphate with microtubule-associated proteins. FEBS Lett 179:289-293

35. Dhamodharan R, Jordan MA, Thrower D, Wilson L, Wadsworth P (1995) Vinblastine suppresses dynamics of individual microtubules in living interphase cells. Mol Biol Cell 6:1215-1229

36. Kreis T, Vale R (1999) Guidebook to the cytoskeletal and motor proteins. Oxford University Press, Oxford

37. Teng J, Wang ZY, Prossnitz ER, Bjorling DE (2008) The G protein-coupled receptor GPR30 inhibits human urothelial cell proliferation. Endocrinology 149:4024-4034

Figure legends

Fig. 1. PCR for GPER1 of tail snips from GPER1 knockout (KO) and wild-type (WT) mice shows a band at the correct size (290 bp) in wild-type but not in knockout mice.

Fig. 2. Treatment with 3 μM G-1 for 24 h under growth-arrested conditions (0% FCS) reduces DNA synthesis in bEnd.3 endothelial cells by about 60%. DNA synthesis was determined by measuring incorporation of [^{3}H]-thymidine (5 μCi) into newly synthesized DNA. The radiolabelled thymidine was present during the last hour of 24 h incubation with G-1. Values are presented as means ±S.E.M. of 5-6 observations in each group. Number of observations represents the number of cell dishes treated with either vehicle or G-1. ** represents $P<0.01$.

Fig. 3. Treatment with 3 but not 1 μM G-1 for 8 days under growth-stimulated conditions (10% stripped FCS) abolishes outgrowth of endothelial cells from mouse aortic rings embedded in Matrigel. G-1 (3 μM) inhibits outgrowth of endothelial cells from aortic rings obtained from three wild-type (A) and three GPER1 knockout mice (B). Please, note that the 3 μM G-1 curve runs close to the X-axis in both panel A and B. The cells growing in Matrigel arranged themselves in tube-like formations. Cell counting was performed by phase contrast microscopy. Values are presented as means ±S.E.M of 7-10 observations. Number of observations represents the number of aortic rings embedded in Matrigel. The experiments were repeated three times. ** and *** represent $P<0.01$ and $P<0.001$, respectively when compared to control.

Fig. 4. Treatment with 3 μM G-1 disrupts mouse bEnd.3 endothelial cell microtubule filaments and causes sharp bends and hooks of the filaments. The microtubule structure was assessed using α-tubulin immunocytochemistry in cells treated with or without 3 μM G-1 for 24 h under growth-stimulated conditions (10% stripped FCS). Fluorescence was analyzed by laser-scanning confocal microscopy on 16 glass cover slips with cells treated with G-1 and on 16 glass cover slips with control cells treated with DMSO as vehicle. These figures show one representative cell out of 35 in each group. Bars represent 5 μm.

Fig. 5. Treatment with G-1 (0.3, 1 and 3 μM) for 24 h under growth-stimulated conditions (10% stripped FCS) alters the microtubule network causing disruptions and sharp bends and hooks of the filaments in a concentration dependent manner in bEnd.3 cells (A) and HUVEC (B). The number of disrupted microtubule per cell was assessed by counting the number of microtubule with sharp bends and hooks in the α-tubulin immunocytochemistry laser-scanning confocal fluorescence microscopy pictures. Summarized data on disrupted microtubule are presented as means ±S.E.M. of 10-35 cells in each group. The figures below the diagrams showing the summarized data depict one representative bEnd.3 cell (two left panels) and HUVEC (two right panels) out of 10-35 in each group. * and *** represent $P<0.05$ and $P<0.001$, respectively, when compared to controls. Bars represent 5 μm.

Fig. 6. Treatment with G-1 (3 μM) for 3 h (A) and 6 h (B) alters the bEnd.3 endothelial cell microtubule network causing disruptions and sharp bends and hooks of the filaments. These figures show one representative cell out of 16-31 in each group. Microtubule was assessed by α-tubulin immunocytochemistry and laser-scanning confocal fluorescence microscopy. Bars represent 5 μm.

Fig. 7. Treatment with G-1 (3 μM) for 24 h alters microtubule structure causing disruptions and sharp bends and hooks of the filaments in the presence of the protein synthesis inhibitor cycloheximide (Cyclo, 50 μg/ml). The figures show one representative cell out of 6-8 in each group. Microtubule was assessed by α-tubulin immunocytochemistry and laser-scanning confocal fluorescence microscopy. Bars represent 5 μm.

Fig. 8. Treatment with G-1 (3 μM) for 24 h under growth-stimulated conditions (10% stripped FCS) disrupts microtubule in aortic smooth muscle cells derived from both wild-type (A) and GPER1 knockout mice (B). These figures show one representative cell out of 10-18 in each group. Microtubule was assessed by α-tubulin immunocytochemistry and laser-scanning confocal fluorescence microscopy. Bars represent 5 μm.

Fig. 9. G-1 stimulates microtubule assembly in-vitro in a concentration-dependent manner. G-1-induced stimulation of microtubule assembly was demonstrated in 3 repeated experiments. Microtubule protein was incubated as described with 0, 10 μM, 25 μM and 50 μM G-1. Microtubule assembly was monitored by measurement of absorbance at 350 nm.

Fig. 1

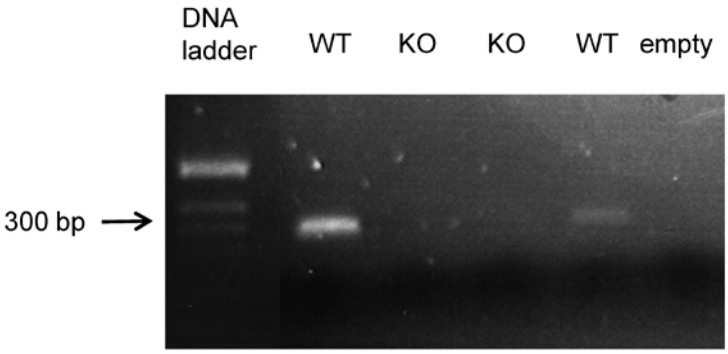

Fig. 2

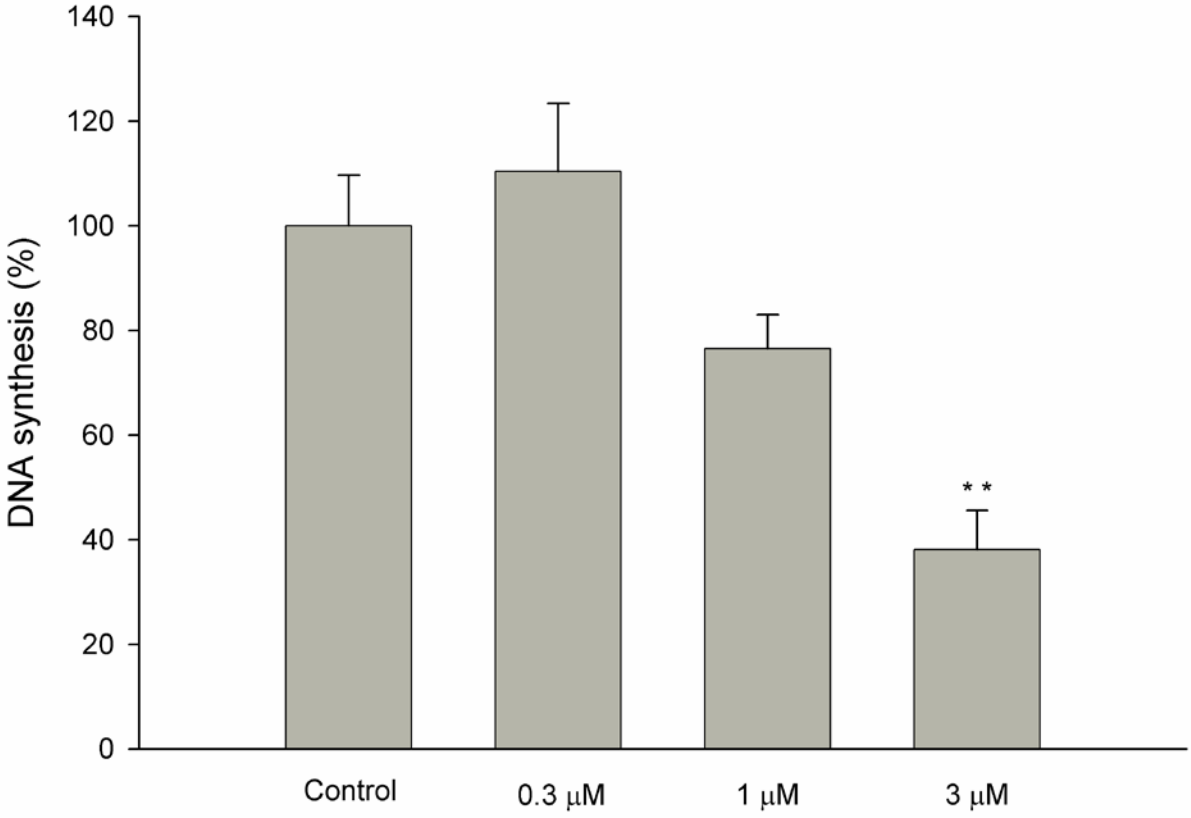

Fig. 3

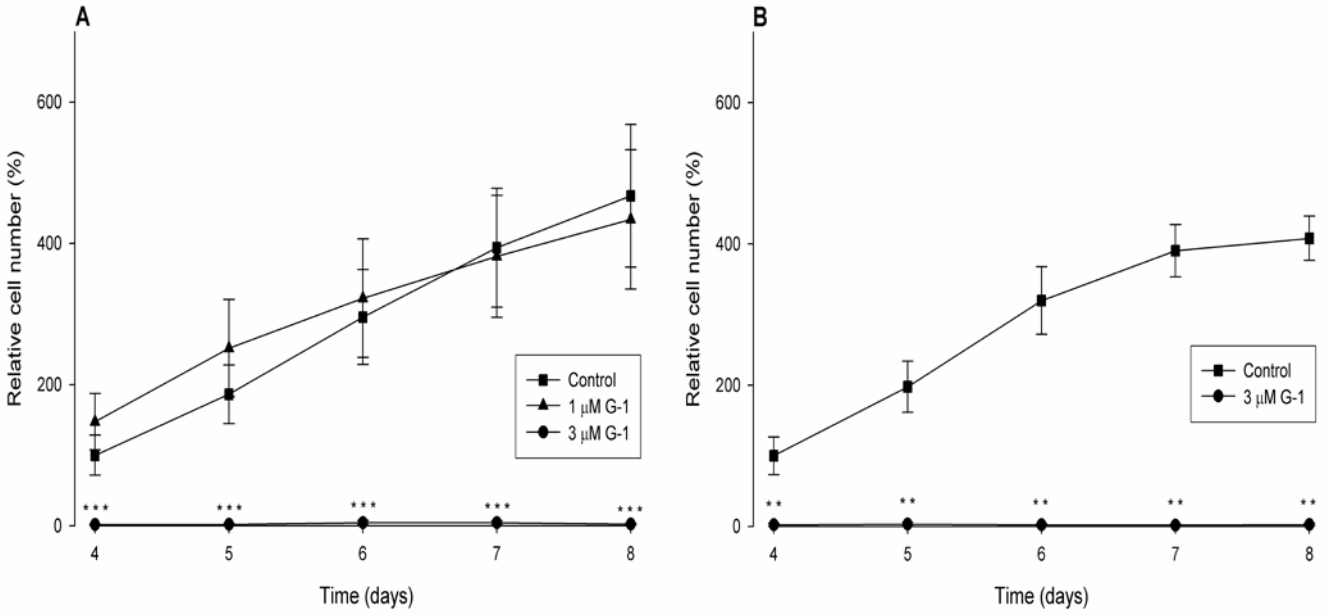
A
Relative cell number (%)
600
400
200
0
4
5
6
7
8
Time (days)
Control
1 μM G-1
3 μM G-1
***
B
Relative cell number (%)
600
400
200
0
4
5
6
7
8
Time (days)
Control
3 μM G-1
**

Fig. 4

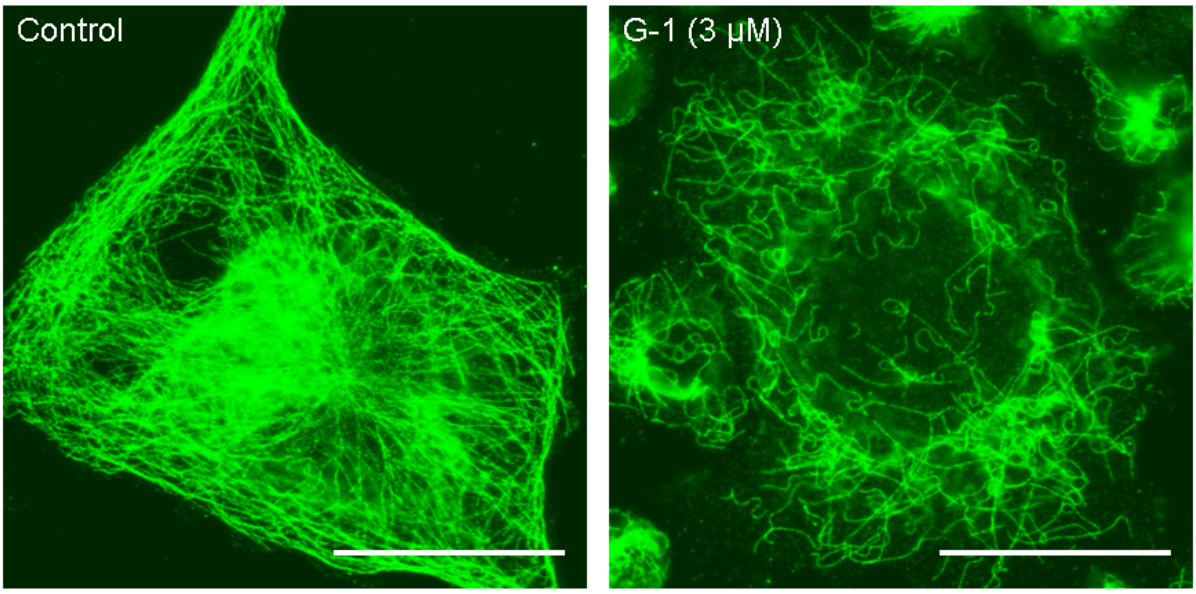

Fig. 5

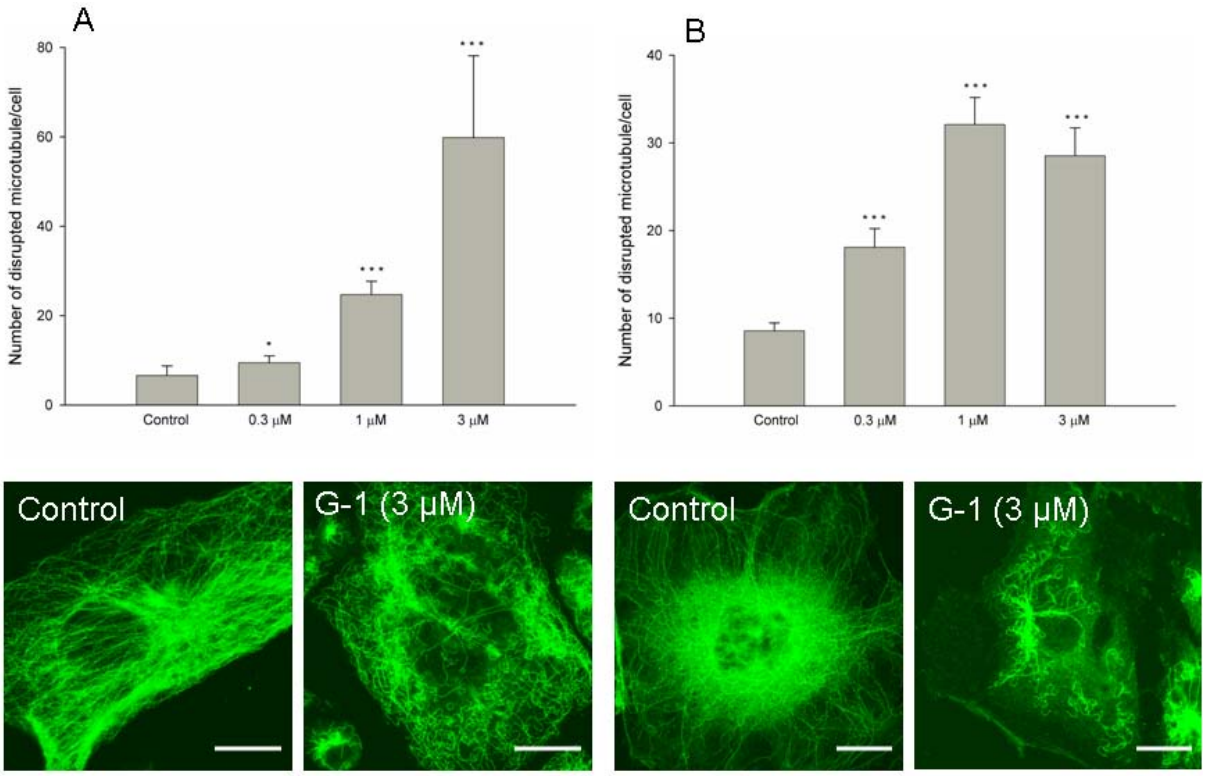
A
Number of disrupted microtubule/cell
80
60
40
20
0
Control
0.3 μM
1 μM
3 μM
B
Number of disrupted microtubule/cell
40
30
20
10
0
Control
0.3 μM
1 μM
3 μM
Control
G-1 (3 μM)
Control
G-1 (3 μM)

Fig. 6

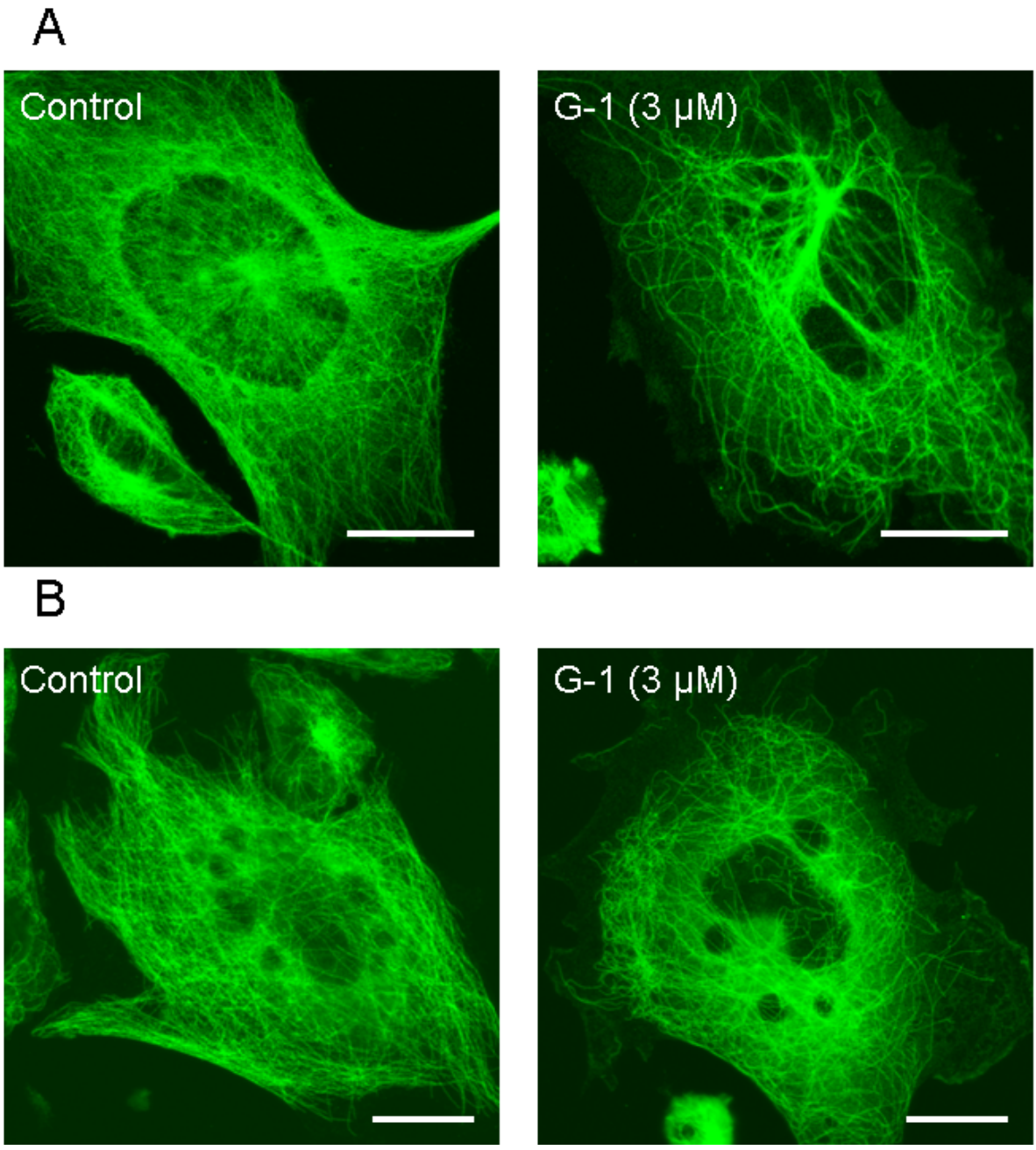

Fig. 7

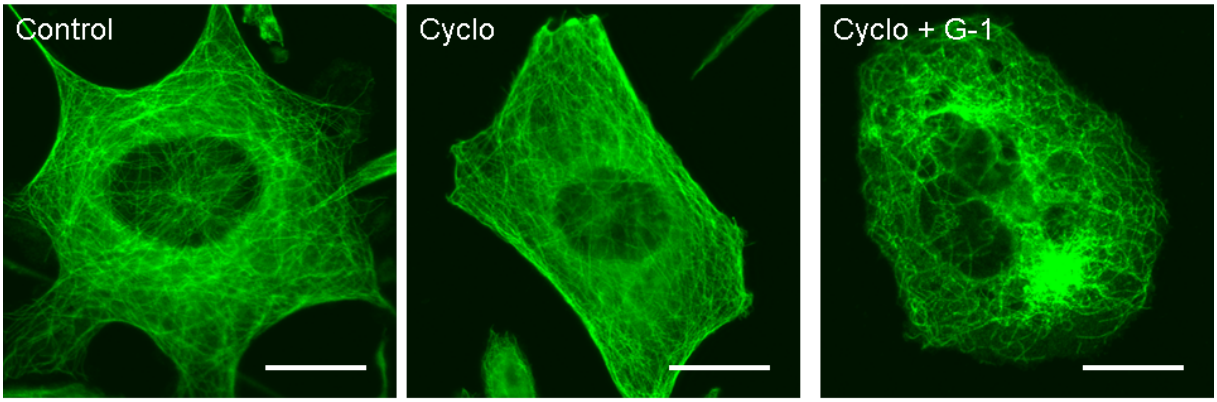

Fig. 8

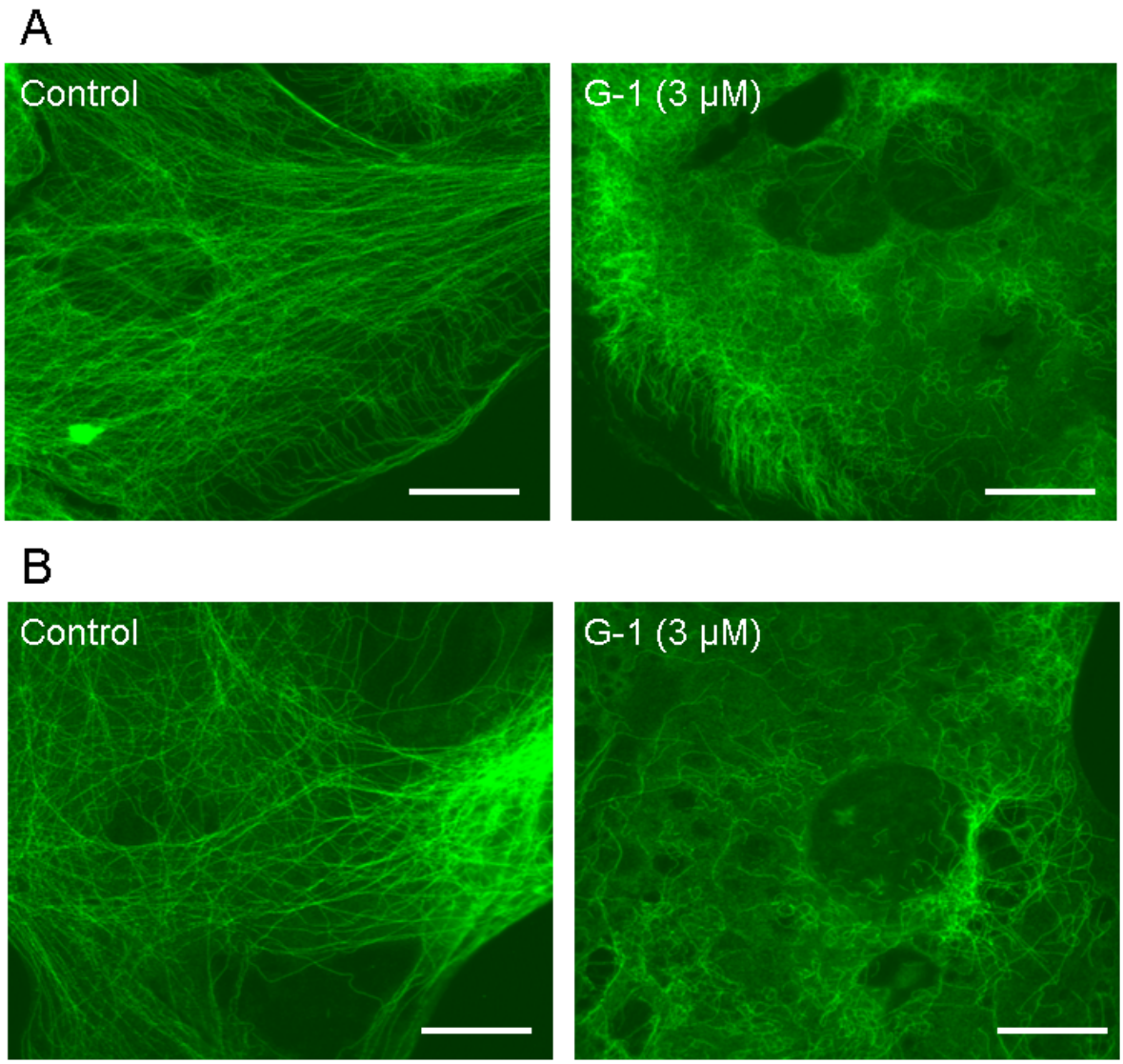

Fig. 9

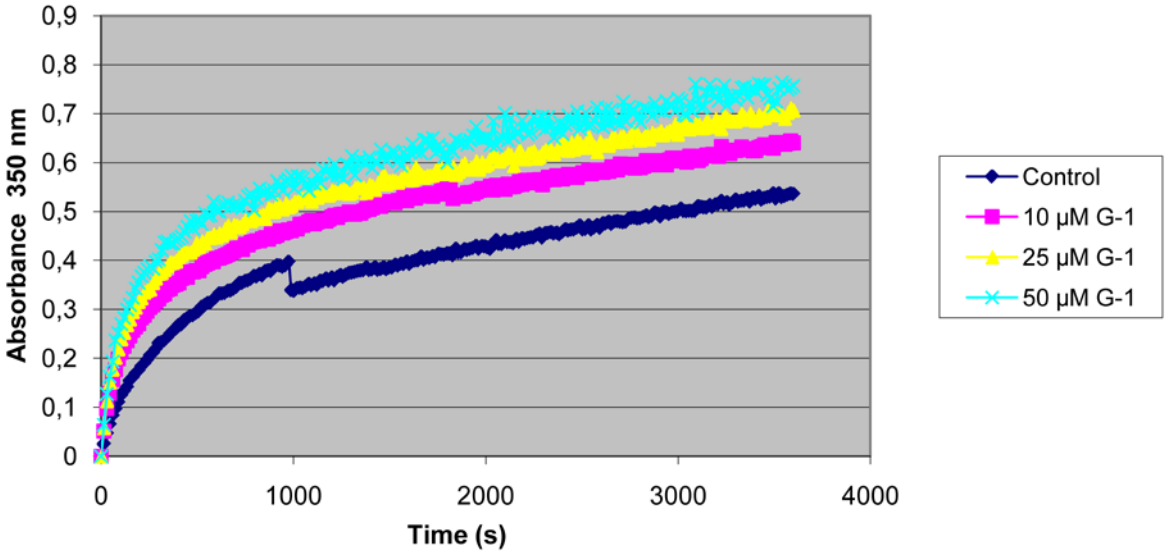
0,9
0,8
0,7
0,6
0,5
0,4
0,3
0,2
0,1
0
Absorbance 350 nm
0
1000
2000
3000
4000
Time (s)
Control
10 µM G-1
25 µM G-1
50 µM G-1